24th COBEM - 2017

24th ABCM International Congress of Mechanical Engineering
December 3-8, 2017, Curitiba, PR, Brazil

COBEM-2017-0488
COMPUTATIONAL ANALYSIS OF THE FLOW AROUND A CANARD TYPE AIRCRAFT

Arthur Octavio Dias dos Santos
Odenir de Almeida
Universidade Federal de Uberlândia, Faculdade de Engenharia Mecânica (FEMEC), Av. João Naves de Ávila, 2121, Uberlândia
arthur@vleaf.com.br ; odenir.almeida@ufu.br

Abstract. *The purpose of this work is to describe the investigation of the aerodynamics characteristics of a canard type aircraft. A numerical analysis was carried out by using Computational Fluid Dynamics (CFD) techniques encountered in STAR-CCM+® commercial software. Each step of this study such as improving the mesh, domain size, turbulence models, and wall treatment was developed and chosen to best perform the simulations at different flight conditions of the aircraft such as takeoff, cruise, landing and pre-stall. The goals of this study was to certify whether CFD can be a reasonable cost effective tool to be used by small enterprises that want to better engineer their designs. After a close analysis of the results, it was verified that only lifting characteristics could be predicted with a reasonable error margin and, for that reason, scaled model should be performed with wind tunnels in order to determine the drag aspects from this specific aircraft.*

Keywords: *canard aircraft, aerodynamics, CFD, RANS, turbulence*

1. INTRODUCTION

Canard airplanes were the pioneers for aircraft designs such as the 14-Bis developed by Alberto Santos Dumont having its first flight in 1906. Despite the fact that these kinds of airplane were the forerunners in aviation they were not produced in large scale in the aeronautical industry until the appearance of the Saab Viggen in 1967 as a jet fighter. Figure 1 illustrates the resurgence of the canard type aircrafts with the SAAB Viggen.

Figure 1. SAAB Viggen J-37 (http://czechairspotters.com/photo.php?id=3276).

Although the aerodynamics of canard airplanes are understood, the majority of the canard aircrafts built nowadays are flying at high speeds such as transonic (0.7 < Mach < 1) or supersonic speeds (Mach > 1). On the other hand, the general aviation branch of aeronautics relates to the airplanes that fly at lower speeds than the commercial airplanes (Mach < 0.7). Aircrafts classified as such have a large spectrum of functions: some are for leisure flights, flight training, emergency medical flights, law enforcement flights, business travels, personal travels, agricultural functions among others applications. The aerospace engineer, Elbert Leander "Burt" Rutan, had a crucial role in the development of canard airplanes for the general aviation market. In the 1970s, he developed the VariViggen a general aviation home-built aircraft that had its name in honor to the Saab Viggen 37. After different variations of the VariViggen such as Long-EZ (also designed by "Burt" Rutan) and Velocity that had great success in its market, the world was around 1970-75 familiarized with canard airplanes. Some designs from Rutan are shown in Fig. 2.

Figure 2. Left (Long-EZ - variation of VariViggen), Right (Velocity Airplane) (http://tinyurl.com/jamstjm; http://tinyurl.com/hzb3rjm).

The aerodynamic design of an aircraft is the key for any new development or incorporation of traditional ideas. In both cases, a good aerodynamic design is aimed to be efficient not only as in fuel efficiency but also in the structural part that are aggregated to the new product. A good aerodynamic design also aims to diminish the drag force and to provide good lift throughout the whole mission (flight-envelop) of the aircraft. Given the importance of aerodynamic for the overall project of any aircraft it is crucial to provide a good analysis of different shapes and aerodynamic configurations expending less time than wind tunnel testing. In the last decades, the numerical wind-tunnel approach via Computational Fluid Dynamics has become an important tool for assessing new aircraft designs and for helping develop more efficient products.

This study will cover the best practices to certify a good aerodynamic analysis making use of the commercial CFD software Star-CCM+®. The motivation for this study rely on the fact that the computational resources have, in the last few years, achieved relatively low prices and may show a good trend of results. They are an affordable mean to perform aerodynamic analysis for micro and medium size business-companies that endeavor to create new aircraft designs such as canard airplanes. In addition, there are very few studies using CFD to evaluate aerodynamics of general aviation canard-aircrafts which made therefore this study to be justifiable from the engineering standpoint.

2. CASE STUDY: CANARD AIRPLANE

The aircraft-object of this study is a canard airplane named Bumerangue EX-27 Cross-Country®. This aircraft is a quadriplace, monoplane, single engine installed in pusher configuration, with retractable landing gear and closed cabin with two access doors in the front. The fuselage is built with composite (fiberglass or Carbon Fiber-main configuration). The powerplant system is composed by a Continental TSIO 360 EB Turbo® – air refrigerated developing 210 HP at 2700 rpm and equipped with a MT propeller® with stainless steel protection and fiberglass. The aircraft is manufactured by FABE – Fabrica Brasileira de Aeronaves located at Uberlandia in the state of Minas Gerais, Brazil. Figure 3 shows the three-views drawing with the main dimensions. Figure 4 illustrates some details of this canard-airplane.

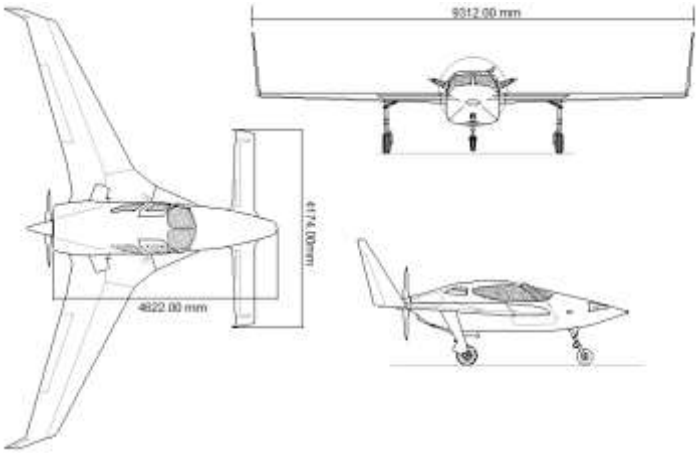

Figure 3. CAD three-view drawing (Courtesy FABE Ltda).

Figure 4. Bumerangue EX-27 Cross-Country® (Courtesy FABE Ltda).

3. NUMERICAL METHODOLOGY

For the present study, a finite volume method was chosen to solve the governing fluid-flow equations in order to calculate the pressure and velocity field for an incompressible and fully developed flow around the aircraft at different flight conditions. The software Star-CCM+ (10.04.009-R8) was used to perform all the calculation necessary to compute lift, drag, lift coefficient, drag coefficient, pressure field, velocity field and other variables to characterize the external aerodynamic analysis of the Bumerangue EX-27 Cross Country®.

The aircraft geometry was drawn using CATIA V5® technical software to provide the external loft of the fuselage, main wing and canard. Later, this geometry was exported to the ANSYS ICEM CFD® to start the process of meshing the surface and volumetric domain. Details of domain size, boundary conditions and meshes are given in the next sub-sections.

3.1 Domain Size, Boundary Conditions and Mesh

When performing aerodynamics simulation it is important to certify that the computational domain drawn around the geometry does not have any interference in the result. This analysis is the first point that has to be validated in order to achieve results with no domain/boundary condition interference. The domain used for this study is a semi-spherical domain. The characteristic length of the airplane is $L = 4.6220\ [m]$. As in Vos (2006) and confirmed by other authors, to have a result with no domain/boundary condition interference, the size of the computational domain must have a diameter of at least 10 times the characteristic length of the body. Figure 5 shows the size of the domain simulated. It is important to say that other three different domain sizes were investigated in this work; however, due to brevity only the results obtained with the domain in Fig. 5 will be presented, since it gave the best compromise between processing time and final result.

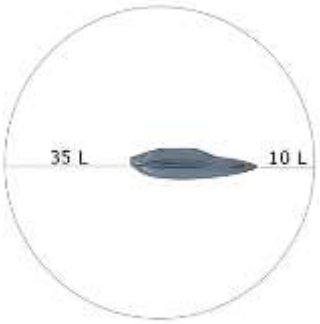

Figure 5. Best domain size for simulations – not in scale.

A tridimensional mesh was created using the software ANSYS ICEMCFD®. The mesh parameters are summarized in table 1. Figure 6 exhibits the mesh built having the symmetry-plane represented in blue and an auxiliary-plane in grey. The auxiliary-plane was used evaluate the quality of the volumetric mesh close to the wing.

The mesh was separated into six regions (Symmetry Plane, Wing, Fuselage, Canard, Winglet and Far-field). Each of these regions had different boundary conditions. The wing, fuselage, winglet and canard regions were separated, so they could have different element sizes for the mesh, allowing the mesh to better represent the leading edge and wing-profile improving the quality of the whole mesh. Their boundary condition was set to *wall* or *no-slip* condition. The Far-field region or the outside shell of the semi-spherical domain was set to *Velocity Intake* condition i.e. the half-shell had the velocity set to a constant, the operational speed of the aircraft. A summary of the software setup is described in table 2:

Table 1. ICEMCFD Setup for Meshing.

Type	**Tetrahedral/Pyramidal/Prisms**
Max Element Size (Farfield)	$10^{7} mm$
Max Element Size Wing & Canard	50
Max Element Size Winglet	60
Number of Density Entities	21
Number of Prism Layers	22
Height of First Prism Layer	0.2
Total Prism Layer Height	54 mm
Prism Layer Growth ratio	1.2
Minimum Quality (ICEM) Pré-Prism Layers	0.35

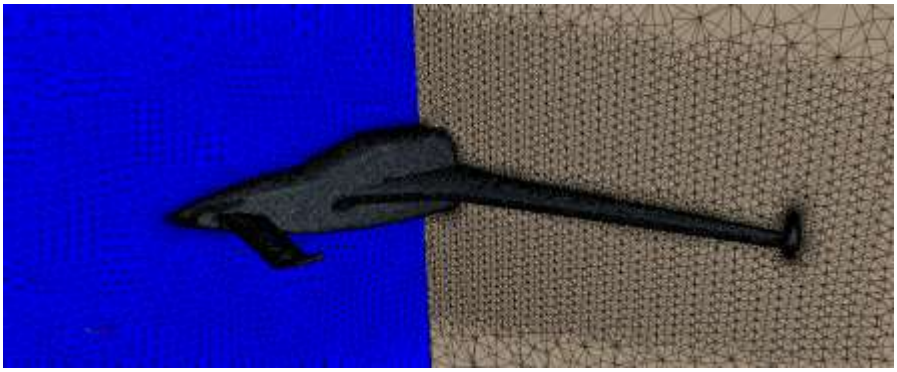

Figure 6. Mesh Example (Symmetry plane in blue; Auxiliary plane in grey).

Table 2. Summary of Star-CCM+ Setup.

Three-Dimensional (3D)
Steady (RANS)
Constant density
Segregated Flow
Turbulent
Sparlat-Allmaras (default Eq. constants)
All y+ Wall Treatment
$V_{cruise} = 200\ kts = 87.45556\ m/s$
$V_{Ref-Turb} = 8.745556\ m/s$
$\nu_{Turb-ratio} = 10$

3.2 Turbulence Modeling

Given the transient nature of the problem related to the flow instability, the solution has to take into account the influence of the flow variations related to the turbulence. The main parameter to check if the flow has or not turbulent behavior is the Reynolds number. It relates the degree of influence of inertial forces over the viscous forces i.e, whether the flow suffers great or few influence of its viscosity. For this study, one flow condition was used in order to standardize the analysis. The cruise condition Reynolds number is:

$$Re_{L-cruise} = \frac{U \cdot L}{\nu} = \frac{87.4556 \cdot 4.622}{1.8705 \cdot 10^{-5}} = 2.610 \cdot 10^{7} \quad (1)$$

A reference value largely used at the literature for external aerodynamic flow is that air flows with Reynolds numbers higher than 5×10^{5} can be considered fully turbulent. Hence, the flow at cruise condition is turbulent and can be modeled as such. The Spalart-Allmaras (1992), at first, emerged due to the necessity of complex flow simulations

mainly in the external aerodynamics for aerospace applications area. Accordingly to Lorin et al (2006) this model consists in an empiric modeling of the production, trip, diffusion and destruction terms of the turbulent viscosity in the flow. This model was designed to external aerodynamic applications where there is free-stream, walls interaction with high Reynolds Number and laminar regions. This turbulence model was selected to perform the simulations. Although other turbulence model (k-ω SST) was evaluated, the results obtained were very similar to the Sparlat-Allmaras, despite the fact the simulation time was bigger – Santos (2017). Such results will not be shown in this paper.

3.3 Numerical Validation

Before proceeding with the main simulations for the canard-airplane, a numerical validation of the software was applied with a similar aerodynamics problem. A set of published experimental data were previously chosen in order to validate the numerical simulations carried out with the software Star-CCM+®. Using the experience obtained from a number of simulations using the software, an ideal mesh was applied to simulate various angles of attack (AOA) and compare the force coefficients such as lift and drag to match the experiment done by Pátek and Smrcek (1999) with a multi-surface aircraft configuration. The geometry chosen from this experimental study was: low-canard wing configuration ($h_{wc} = 4\ c; v_{wt} = 0$), there was no horizontal tail in this configuration. Figure 7 illustrates the different configurations performed by Pátek and Smrcek (1999). Figure 8 shows the configuration and the mesh applied to the simulations with Star-CCM+®.

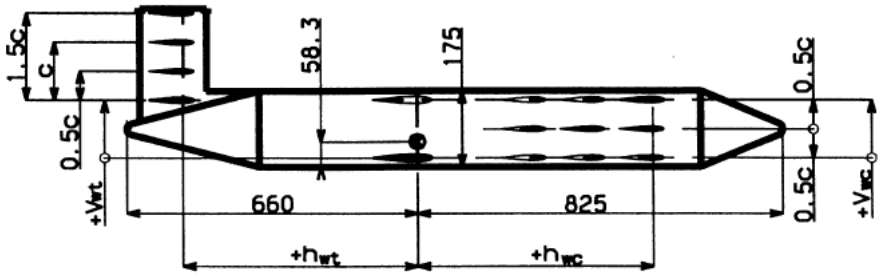

Figure 7. Different configurations performed in the experiment from Pátek and Smrcek (1999).

The mesh was built following the same procedure as described in the numerical methodology. In this case, the semi-spherical domain had a diameter of 10 times the characteristic length of the geometrical model ($L = 1.485$ m). The final number of cells reached about 5 million with the inclusion of prism layers.

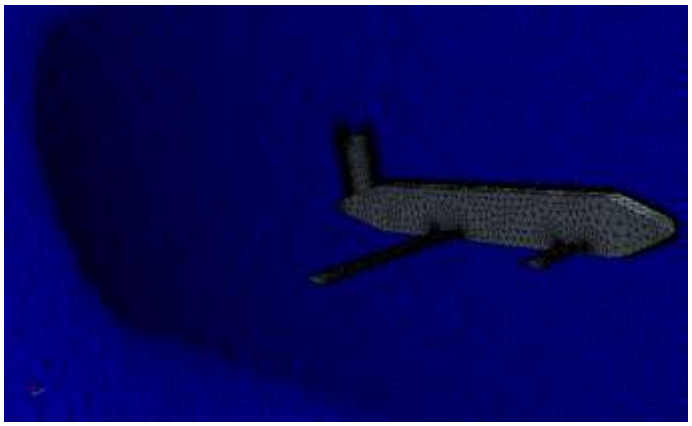

Figure 8. Mesh details for the multi-surface validation case.

Considering the wind tunnel used for the experiment (1.8 m low-speed wind tunnel at VZLU, Aeronautical Research and Test Institute in Prague) the Reynolds number based on the wing chord was 3.35×10^5. The chord of the aircraft model is $c = 100$ mm then resulting in a velocity of $U = 48.7869$ m/s.

The simulations were run with the use of the Spalart-Allmaras turbulence model and the setup according to the Table 2, changing the value of the flight-velocity condition and including the different angles of attack (AOA).

4. NUMERICAL RESULTS

In the next sub-sections are presented the numerical validation results and the simulations for the Bumerangue EX-27 at two different flight conditions investigated. The numerical validation was consistent with the data available from the work of Pátek and Smrcek (1999) with focus to the lift-curve. The simulations for the canard-airplane were focused to the pressure coefficient distribution and evaluation of lift and drag. No experimental data is available for the real airplane configuration.

4.1 Numerical Validation Results

A set of simulations were performed with multi-surface configuration at different AOA varying from -2º up to 10º. The parameters that will be compared are the lift and drag coefficient. Figure 9 shows the plot comparison between experiment data and simulation of the model for the CL versus AOA.

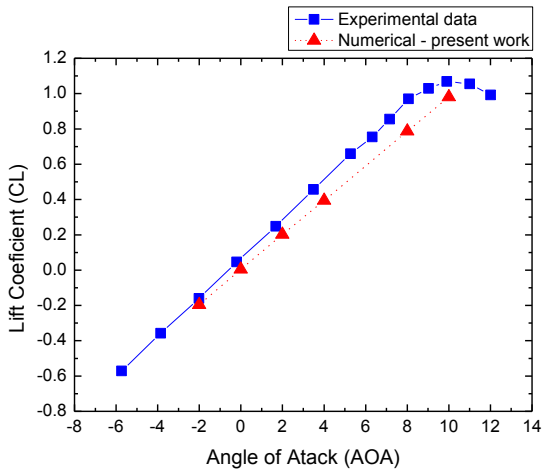

Figure 9. Results comparison (Lift coefficient vs Angle of Attack).

As illustrated in Fig. 9 the numerical data is following closely the experimental points at low angles of attack up to 8º. After this point, it is noticed some lack of agreement, mainly due to viscous effects since part of the flow over the canard is "stalled". Despite the fact that the lift-value in the linear region (smooth flow) is reasonable it is expected a limited evaluation for the aerodynamic drag. Figure 10 presents this results confirming that the aerodynamic drag is not well captured by the present simulations.

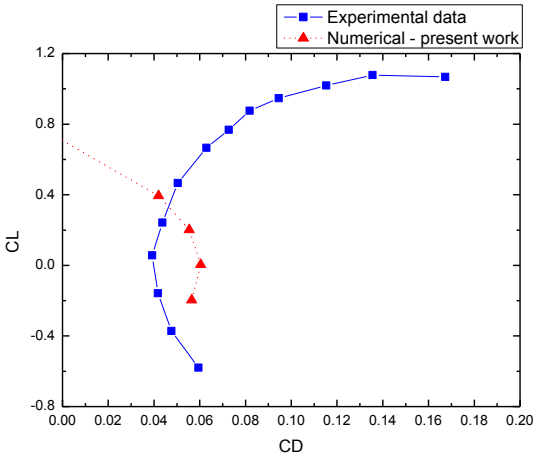

Figure 10. CL vs CD curve comparison.

It is understood that to capture the correct flow pattern under the viscous effect in the separation zone over the canard and main wing, a more refined mesh is required. The results presented herein are not showing the limitation of the software, but confirming the fact that the lift prediction is much less influenced by the viscous effect and that for a reasonable aerodynamic evaluation the inclusion of a lot of points close to the wall is mandatory. Moreover, it is important to point out the influence and the capability of the turbulence model to tackle transition and complete flow detachment over the surface. All these variables put together are limiting the analysis presented in this study.

Figures 11 and 12 present the contours of velocity and pressure fields evaluated at the symmetry plane for two different AOA. These plots were consistent with the flow pattern expected for the analysis. At low AOA the flow is completely attached to the fuselage, canard and main wing. The wake-flow is seen only at the end of the vertical tail, as seen in Fig.11. As mentioned, the flow separation was identified at the canard and main wing for high AOA.

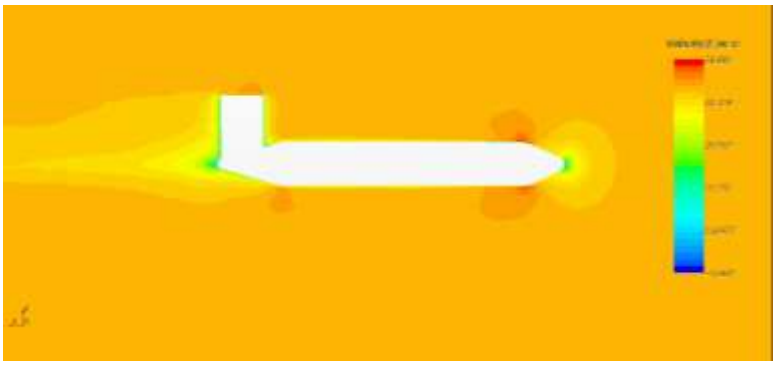

Figure 11. Velocity contour plot at AOA = 0 deg.

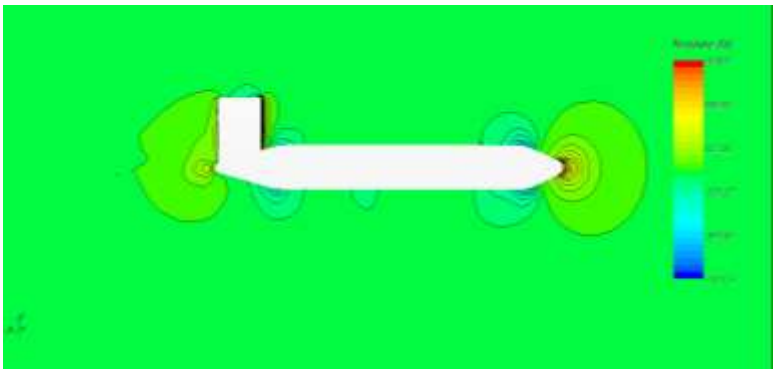

Figure 12. Pressure contour plot at AOA = 6 deg.

4.2 Numerical Results - Canard

The numerical results for the canard-airplane were based on the pressure coefficient distribution along two different canard and wing sections and values for lift and drag aerodynamics coefficients. Figure 13 illustrates the aircraft model with the highlighted location for mid-wing and mid-canard where the profiles were taken. The first position was 2.2 meters from the origin of the model in the Y direction (Mid-wing); the second position was located 1.2 meter from the origin of the model in the Y direction as well (Mid Canard).

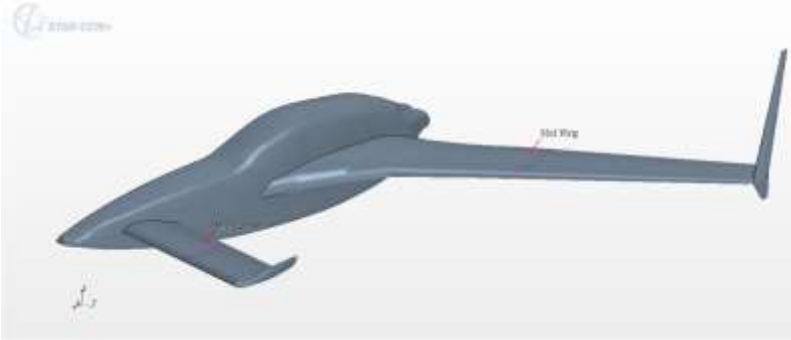

Figure 13. Location of the pressure coefficient (cp) profiles.

According to the guideline from the aircraft-manufacturer a matrix of operational conditions was developed in order to have results that could be further studied experimentally in wind tunnels and also in flight tests. Table 3 describes each flight condition accordingly with its reference values for velocity, pressure and angle of attack.

Table 3. Operational Conditions Simulated

Flight Condition	Velocity [m/s]	Pressure [Pa]	Angle of Attack [deg]
Take-off	38.5833	101325	2
Cruise	87.4556	69820.0	0

For each flight condition simulated, the parameters collected as results were: lift, drag, lift coefficient, drag coefficient, pressure coefficient, velocity field and pressure field. These data will be presented in the next sub-sections.

4.3 Numerical Results – Take-off condition

The take-off condition imposed a different model to be simulated since the elevator (attached to the canard) is normally deflected in that condition. The condition simulated had the elevator deflected 15 degrees. The introduction of the elevator increased the complexity of the flow over the canard with flow detaching of it in the rearward part of the canard (above the elevator). This flow pattern led to some oscillations of velocity in the region making it harder to average by doing RANS simulations. Figure 14 and 15 shows the pressure difference (pressure coefficient) between upper and lower part of both mid-canard and mid-wing profiles. In Fig. 14 the cp-curve is opened at the trailing edge, suggesting that the steady-state solution was not reproducing the physics of the problem. This problem was solved increasing the number of points in the trailing edge region and the quality on the canard surface cells to register all the pressure variations with accuracy.

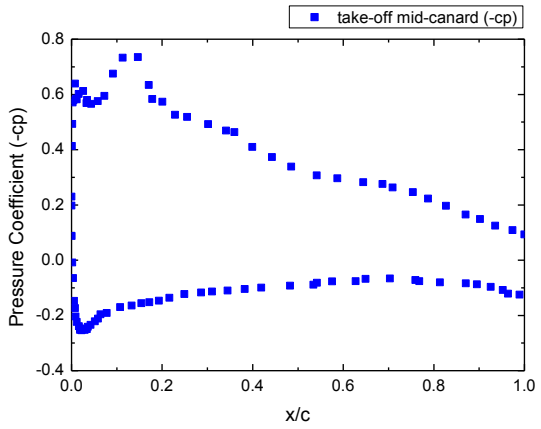

Figure 14. Plot of pressure coefficient at Takeoff condition at the mid-canard profile.

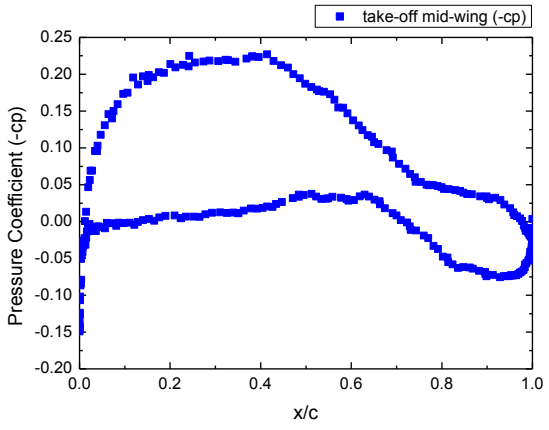

Figure 15. Plot of pressure coefficient at Takeoff condition at the mid-wing profile.

Figure 16 describes the velocity contours and pathlines for the flow around the canard-airplane flying at the take-off condition. Due to the angle of attack (AOA = 2º) the flow is coming upward in the front wing, where it is possible to visualize the tip-vortex from the canard affecting the main flow over the wing.

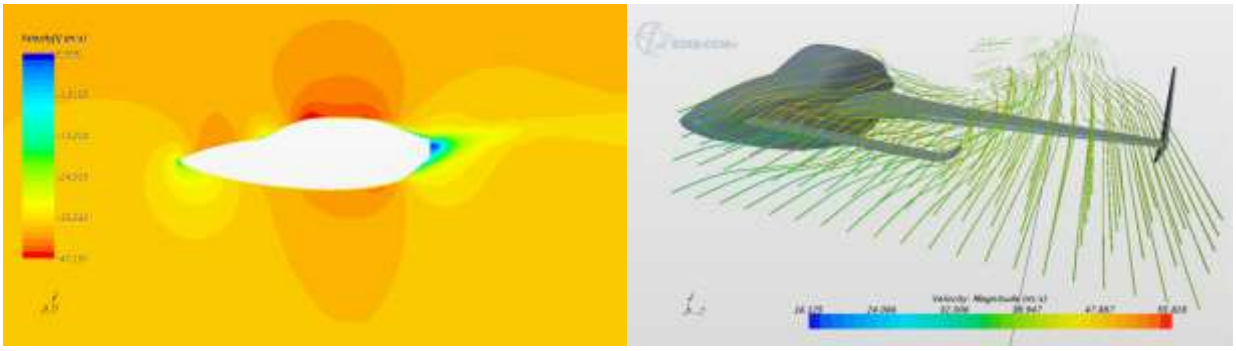

Figure 16. Velocity contours and pathlines – take-off condition.

4.4 Numerical Results – Cruise condition

The cruise condition is very important for the preliminary studies of any aircraft, since the airplane remains most of the mission-time in this situation. By analyzing this flight-condition it is expected to capture at least the lift distribution over the main wing with reasonable accuracy. Figure 17 and 18 shows the pressure coefficient plot for both mid-canard and mid-wing profiles at cruise condition.

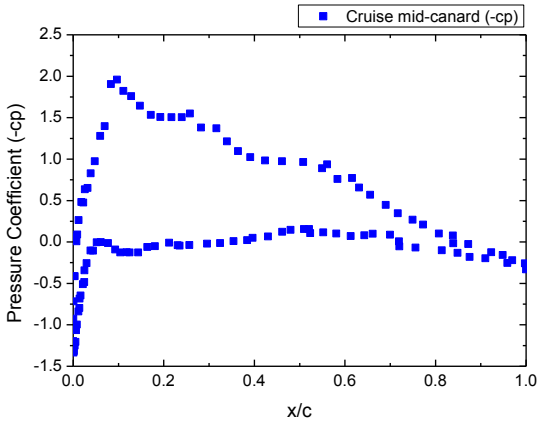

Figure 17. Plot of pressure coefficient at Cruise condition at the mid-canard profile.

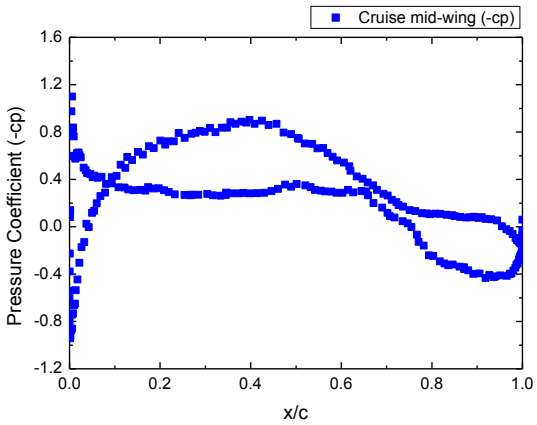

Figure 18. Plot of pressure coefficient at Cruise condition at the mid-wing profile.

Due to the steady-state characteristic of this flow condition, the cp-profiles are well defined providing reasonable values for the lift force for the airplane. Despite the fact that these data must be corroborated by experiments, it is believed that design trends could apply by considering some of the results obtained in this numerical investigation.

Figure 19 describes the velocity contours and pathlines for the flow around the canard-airplane flying at the cruise condition. In this case the flow is well-organized and the tip-vortex from the canard is barely affecting the main flow over the wing.

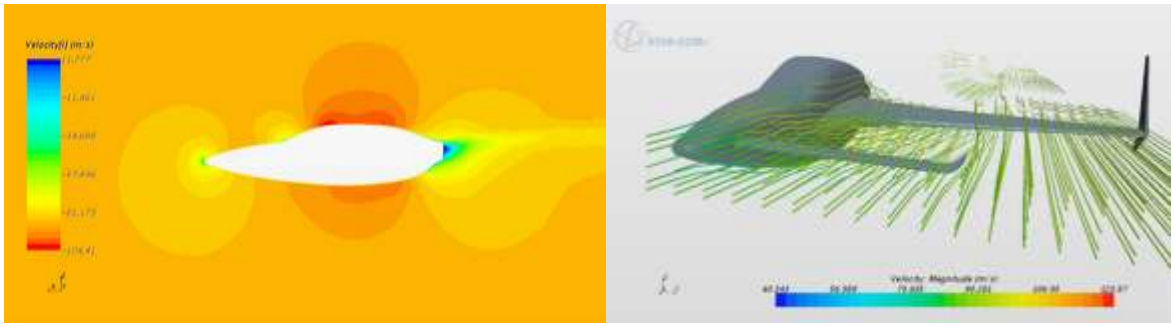

Figure 19. Velocity contours and pathlines – cruise condition.

Finally, Table 4 presents the numerical values obtained for the lift and drag coefficients for the current simulations. As mentioned before, the absolute values of these quantities must be corroborated by experiments, however, it is expected that at least the lift trends are captured by the present simulations.

Table 4. Lift and Drag coefficients – numerical results.

Flight Condition	Cl	Cd
Take-off	0.485170	0.0049222
Cruise	0.232052	0.0226350

5. CONCLUSIONS

The CFD analysis of a canard airplane was performed with relatively accuracy using hybrid meshes. The work done also showed that the CFD analysis using resources relatively inexpensive compared to supercomputers could help to drive trends and other important characteristics from the aerodynamics of such airplanes presenting itself as a reasonable solution for small aviation entrepreneurs. Issues like mesh sizing and the choice of turbulence modeling could affect the accuracy of the final solution, especially in those conditions were part of the flow is detached from aircraft surfaces. One of the possibilities to improve the solution is to use hexahedral mesh to discretize the airplane, however such approach could lead to very complex topologies. The validation and simulations with the real airplane were satisfactory, showing some trends and patterns encountered in this type of flow. Despite the fact that the lift could be predicted in the linear region of the CL × α curve, the lack of points and probably the turbulence modeling affected the drag prediction. Scaled model experiments in wind tunnel would help to evaluate the drag from this airplane and led to further improved simulations. At the end, the numerical analysis showed good prediction of lift. For Future work improvements in the drawings of the primary lifting surfaces as elevator, ailerons and winglets should be added and simulated as well so other maneuvers could be tested and certify all the forces within the airframe of the aircraft.

6. ACKNOWLEDGEMENTS

The authors would like to thank the CPAERO (Experimental Aerodynamics Research Center) for all support during the execution of this work. Also, the authors recognize the support of Fundação de Amparo a Pesquisa do Estado de Minas Gerais – FAPEMIG.

7. REFERENCES

Vos, W. 2006. The Verification and Validation of Preliminary CFD Results for the Construction of an A Priori Aerodynamic Model. Delft, Netherlands.

R., S. P. 1992. "A one equation turbulence model for aerodynamic flows". Reno , NV, January 1992.: AIAA 30th Aerospace Sciences Meeting and Exhibit.

Lorin, E., Amine Ben Haj Ali, U. d., E. d., Azzeddine Soulaimani, E. d. 2006. "An accurate positivity preserving scheme for the Spalart-Allmaras turbulence model". San Francisco, California: 36th AIAA Fluid Dynamics Conference and Exhibit.

Santos, A.O.D., 2016. “Aerodynamics CFD Analysis of a Canard Type Aircraft (Bumerangue EX-27)”. Undergraduate project, Federal University of Uberlândia, Uberlândia, MG, Brazil.

Pátek, Z., Smrcek, L. 1999. "Aerodynamic characteristics of multi-surface aircraft configurations". Aircraft Desing, Vol. 2, Issue 4, pp. 191-206, Glasgow, Scotland, UK.

8. RESPONSIBILITY NOTICE

The author(s) is (are) the only responsible for the printed material included in this paper.